A&A 608, A19 (2017)
DOI: 10.1051/0004-6361/201730588

Astronomy & Astrophysics

"TNOs are Cool": A survey of the trans-Neptunian region

XIII. Statistical analysis of multiple trans-Neptunian objects observed with *Herschel* Space Observatory⋆

I. D. Kovalenko[1,5], A. Doressoundiram[1], E. Lellouch[1], E. Vilenius[2], T. Müller[3], and J. Stansberry[4]

[1] LESIA, Observatoire de Paris, PSL Research University, CNRS, Sorbonne Universités, UPMC Univ. Paris 06, Univ. Paris Diderot, Sorbonne Paris Cité, 5 place Jules Janssen, 92195 Meudon Principal Cedex, France
e-mail: irina.kovalenko@obspm.fr
[2] Max-Planck-Institut für Sonnensystemforschung, Justus-von-Liebig-Weg 3, 37077 Göttingen, Germany
[3] Max-Planck-Institut für extraterrestrische Physik (MPE), Giessenbachstrasse, 85748 Garching, Germany
[4] University of Arizona, 85721 Tucson, USA
[5] Institute of Astronomy, Russian Academy of Sciences, Pyatnitskaya 48, 119017 Moscow, Russia

Received 9 February 2017 / Accepted 18 September 2017

ABSTRACT

Context. Gravitationally bound multiple systems provide an opportunity to estimate the mean bulk density of the objects, whereas this characteristic is not available for single objects. Being a primitive population of the outer solar system, binary and multiple trans-Neptunian objects (TNOs) provide unique information about bulk density and internal structure, improving our understanding of their formation and evolution.
Aims. The goal of this work is to analyse parameters of multiple trans-Neptunian systems, observed with *Herschel* and *Spitzer* space telescopes. Particularly, statistical analysis is done for radiometric size and geometric albedo, obtained from photometric observations, and for estimated bulk density.
Methods. We use Monte Carlo simulation to estimate the real size distribution of TNOs. For this purpose, we expand the dataset of diameters by adopting the Minor Planet Center database list with available values of the absolute magnitude therein, and the albedo distribution derived from *Herschel* radiometric measurements. We use the 2-sample Anderson–Darling non-parametric statistical method for testing whether two samples of diameters, for binary and single TNOs, come from the same distribution. Additionally, we use the Spearman's coefficient as a measure of rank correlations between parameters. Uncertainties of estimated parameters together with lack of data are taken into account. Conclusions about correlations between parameters are based on statistical hypothesis testing.
Results. We have found that the difference in size distributions of multiple and single TNOs is biased by small objects. The test on correlations between parameters shows that the effective diameter of binary TNOs strongly correlates with heliocentric orbital inclination and with magnitude difference between components of binary system. The correlation between diameter and magnitude difference implies that small and large binaries are formed by different mechanisms. Furthermore, the statistical test indicates, although not significant with the sample size, that a moderately strong correlation exists between diameter and bulk density.

Key words. Kuiper belt: general – methods: statistical

1. Introduction

Within the "TNOs are Cool: A Survey of the Trans-Neptunian Region" program (Müller et al. 2009) more than 30 multiple objects have been observed. The thermal emission measurements, provided by the *Herschel* Space Observatory (Pilbratt 2008), allowed to obtain important physical properties, such as radiometric size and albedo. In the present paper we describe a statistical analysis of the obtained properties, looking for unique aspects of the size and albedo distributions for trans-Neptunian objects (TNOs) with satellites as compared with those for single TNOs.

The study of TNOs with satellites has an important advantage over single TNOs, since the mass can be derived from satellite orbit, using Kepler's third law. Giving the radiometric size and mass the mean bulk density of the objects can be estimated. This later crucial parameter contains information on both internal structure (i.e. differentiation and/or layering porosity) and chemical composition (i.e. rock/ice). An analysis of the obtained size and albedo on possible correlation with the bulk density and other physical and orbital parameters is carried out. Since the probability distributions of parameters are unknown, non-parametric statistical methods are applied.

The structure of the paper is as follows. In Sect. 2 we describe the dataset, used for the statistical analysis. In Sect. 3, we compare two populations – multiple and single TNOs, applying non-parametric test on size distributions. The bulk density estimation is done in Sect. 4. The analysis on correlations of physical and orbital parameters, characterising multiple TNOs, is performed in Sect. 5. Section 6 summarises results of statistical analysis.

2. Dataset

Our analysis is based on the data obtained during the "TNOs are cool" program, which contains 28 binary and 2 triple systems

⋆ *Herschel* is an ESA space observatory with science instruments provided by European-led Principal Investigator consortia and with important participation from NASA.

Table 1. Dataset.

Object	Dyn. cl.	D, km	p_V	Reference	ΔH_V	$m \times 10^{18}$, kg	ρ_b, g/cm^3
2001 QY297	CC	229^{+22}_{-108}	$0.152^{+0.439}_{-0.035}$	Vilenius et al. (2014)	0.2	4.105 ± 0.038^a	$0.92^{+1.31}_{-0.27}$
2001 XR254	CC	221^{+41}_{-47}	$0.136^{+0.168}_{-0.044}$	Vilenius et al. (2014)	0.43	4.055 ± 0.065^a	$1.00^{+0.98}_{-0.57}$
Borasisi	CC	163^{+32}_{-66}	$0.236^{+0.438}_{-0.077}$	Vilenius et al. (2014)	0.45	3.433 ± 0.027^a	$2.1^{+2.6}_{-1.2}$
Teharonhiawako	CC	220^{+41}_{-44}	$0.145^{+0.086}_{-0.045}$	Vilenius et al. (2014)	0.7	2.445 ± 0.032^a	$0.60^{+0.36}_{-0.33}$
2005 EF298	CC	174^{+27}_{-32}	$0.16^{+0.13}_{-0.07}$	Vilenius et al. (2012)	0.59	2.2 ± 0.1^b	$1.10^{+0.66}_{-0.56}$
Sila-Nunam	CC	343 ± 42	$0.090^{+0.027}_{-0.017}$	Vilenius et al. (2012)	0.12	10.84 ± 0.22^c	0.72 ± 0.28
2001 RZ143	CC	140^{+39}_{-33}	$0.191^{+0.066}_{-0.045}$	Vilenius et al. (2012)	0.4	–	–
2003 QA91	CC	260^{+30}_{-36}	$0.130^{+0.119}_{-0.075}$	Vilenius et al. (2014)	0.1	–	–
2003 QR91	CC	280^{+27}_{-30}	$0.054^{+0.035}_{-0.028}$	Vilenius et al. (2014)	0.2	–	–
2003 WU188	CC	<220	>0.15	Vilenius et al. (2014)	0.7	–	–
2002 VT130	CC	324^{+57}_{-68}	$0.097^{+0.098}_{-0.049}$	Mommert (2013)	0.44	–	–
Makemake^k	HC	1440 ± 9	0.77 ± 0.03	Ortiz et al. (2012)	7.8	2600 ± 500^k	1.7 ± 0.36
Salacia	HC	901 ± 45	0.044 ± 0.004	Fornasier et al. (2013)	2.36	436 ± 11^d	1.29 ± 0.23
Haumea^l	HC	1240^{+69}_{-59}	$0.804^{+0.062}_{-0.095}$	Fornasier et al. (2013)	2.98	4030 ± 40^e	$2.55^{+0.1}_{-0.01}$
Altjira	HC	331^{+51}_{-187}	$0.043^{+0.1825}_{-0.0095}$	Vilenius et al. (2014)	0.23	3.99 ± 0.067^a	$0.30^{+0.51}_{-0.14}$
Varda	HC	792^{+91}_{-84}	$0.102^{+0.024}_{-0.020}$	Vilenius et al. (2014)	1.45	265 ± 3.9^b	$1.27^{+0.41}_{-0.44}$
Quaoar^m	HC	1110 ± 5	0.109 ± 0.007	Braga-Ribas et al. (2013)	5.6	1400 ± 210^f	1.99 ± 0.46
2002 UX25	HC	697^{+23}_{-25}	$0.107^{+0.005}_{-0.008}$	Fornasier et al. (2013)	2.5	125 ± 3^g	0.79 ± 0.10
2001 QC298	HC	303^{+27}_{-30}	$0.061^{+0.027}_{-0.017}$	Vilenius et al. (2014)	0.44	11.88 ± 0.14^a	$1.14^{+0.34}_{-0.3}$
Orcus	Plu	958 ± 23	$0.231^{+0.018}_{-0.011}$	Fornasier et al. (2013)	2.61	636 ± 3.3^a	$1.53^{+0.12}_{-0.12}$
1999 TC36	Plu	393^{+25}_{-27}	$0.079^{+0.013}_{-0.011}$	Mommert et al. (2012)	2.21	12.8 ± 0.06^h	$0.62^{+0.13}_{-0.12}$
2003 AZ84	Plu	727^{+62}_{-67}	$0.107^{+0.023}_{-0.016}$	Mommert et al. (2012)	5	–	–
Huya	Plu	458 ± 9	0.083 ± 0.004	Fornasier et al. (2013)	1.56	–	–
2002 WC19	Res	348 ± 45	$0.167^{+0.052}_{-0.037}$	Lellouch et al. (2013)	3.1	77 ± 5^b	3.47 ± 1.7
1998 SM165	Res	291^{+22}_{-26}	$0.083^{+0.018}_{-0.013}$	Lellouch et al. (2013)	2.69	6.89 ± 0.01^a	$0.59^{+0.16}_{-0.13}$
Typhon	SDO	185 ± 7	0.044 ± 0.003	Santos-Sanz et al. (2012)	1.3	0.87 ± 0.03^d	0.33 ± 0.05
Ceto	SDO	281 ± 11	0.056 ± 0.006	Santos-Sanz et al. (2012)	0.58	5.41 ± 0.42^i	0.64 ± 0.13
Eris^n	Det	2260 ± 50	$0.96^{+0.09}_{-0.04}$	Sicardy et al. (2011)	6.7	16700 ± 200^j	2.75 ± 0.22
1995 TL8	Det	244^{+82}_{-63}	$0.231^{+0.189}_{-0.102}$	Lellouch et al. (2013)	1.7	–	–
2007 UK126^n	Det	614 ± 15	$0.15^{+0.016}_{-0.016}$	Schindler et al. (2017)	3.79	–	–

Notes. Diameter D and albedo p_V are obtained by applying the hybrid STM or NEATM (Harris 1998; Lebofsky et al. 1986; Stansberry et al. 2008) to the fluxes measured by *Herschel* (and *Spitzer* when are available) for all objects, unless otherwise indicated. Dyn. cl. means dynamical classification: CC denotes cold classicals, HC denotes hot classicals, Plu denotes plutinos, Res denotes resonant objects, SDO denotes scatered disc objects, and Det denoted detached objects. Magnitude difference between the primary and secondary, ΔH_V, is from Grundy's tables on webpage[2]. The triple systems Haumea and 1999 TC36 are also considered here as binaries: the magnitude difference between the primary and the most distant satellite is used. Bulk density ρ_b is calculated in this work, unless otherwise indicated (see text). System mass, m, is from literature. [(a)] Grundy et al. (2011); [(b)] Grundy's tables on webpage[2]; [(c)] Grundy et al. (2012); [(d)] Stansberry et al. (2012); [(e)] Ragozzine & Brown (2009); [(f)] Fraser et al. (2013); [(g)] Brown (2013); [(h)] Benecchi et al. (2010); [(i)] Grundy et al. (2007); [(j)] Brown & Schaller (2007); [(k)] Size and albedo were obtained from stellar occultation. The effective diameter D is derived with $D_1 = 1430 \pm 14$ km (Ortiz et al. 2012) and $D_2 = 175 \pm 75$ km (Parker et al. 2016). [(l)] Bulk density is from Lacerda & Jewitt (2007), calculated with assumption of Jacobi triaxial ellipsoid form. [(m)] Size and albedo were obtained from stellar occultation. Bulk density is from Braga-Ribas et al. (2013), calculated with assumption of Maclaurin spheroid form. [(n)] Size and albedo were obtained from stellar occultation.

(hereafter we denote them TNBs) and 108 single TNOs. Although, the Pluto system was also observed by *Herschel*, here we have not included it in our analysis because this much more complex system (e.g. with a highly variegated surface) is already being largely described in other publications, for example, by Stern et al. (2015), Lellouch et al. (2016), Grundy et al. (2016), Weaver et al. (2016).

We have adopted dynamical class (according to Gladman et al. (2008) classification), orbital parameters of heliocentric motion, the radiometric diameter (D) and the geometric albedo (p_V) from the literature, mainly from the "TNOs are cool" paper series (see Table 1). These parameters can also be found at the "TNOs are cool" open database[1]. The diameter and albedo were derived from the *Herschel* (and *Spitzer* when available) measurements with the near-Earth asteroid thermal model (NEATM, Harris (1998)) or the hybrid standard thermal model (hybrid STM, Lebofsky et al. (1986), Stansberry et al. (2008)). The difference to the hybrid standard thermal model is that NEATM takes into account emission from the illuminated part of the object only using the

[1] http://public-tnosarecool.lesia.obspm.fr/

Sun-target-observer phase angle, but this is a negligible effect at centaurs/TNOs distance.

A complementary information about magnitude difference between components (ΔH_V) is provided by the open data on W. Grundy's webpage[2]. The information about system mass (when available) is from the literature mentioned in Table 1. Additionally, in this work we have used parameters of mutual orbit (semi-major axis and orbital period) from the same literatures as for masses. The mean bulk density calculation is described in Sect. 4.

3. Two populations comparison

Two populations, multiple and single TNOs, are compared here through their size distributions. The aim is to clarify whether the both populations are similar and come from the same parent-population.

The *Herschel* and *Spitzer* measurements have provided the biggest sample of accurate TNOs sizes, derived from observations at thermal wavelengths. However, regarding the entire TNOs population, this sample is still small and may give an incomplete picture of the real albedo and diameter distributions. In order to avoid or reduce the possible *Spitzer*/*Herschel* selection bias, we expand the data sample, using the Minor Planet Center (MPC) database[3] and applying a Monte Carlo simulation. The MPC provides the list of TNOs, Centaurs and SDO, which contains 2528 objects, where 78 of them are known to be binaries or multiples. We initially start with this full MPC list.

The Monte Carlo sampling of TNOs diameters is performed as follows. For those objects for which the radiometric size is unknown, we assign a diameter using available magnitudes H_V from MPC, and following an albedo distribution. The empirical albedo distribution, assumed to be the same for binaries and single TNOs, is taken from the "TNOs are cool" open database and determined for each dynamical group. For each object we randomly select an albedo value from the corresponding dynamical group sample, while simultaneously varying this value following given uncertainty. This Monte Carlo approach combines resampling and perturbation techniques. The obtained diameters dataset, completed by those objects for which we have the radiometric size, is used for a statistical test, described below, which compares TNBs and TNOs samples. The aforementioned diameters sampling is repeated many times in order to calculate an average test statistic.

In order to test the hypothesis that both samples come from the same but unspecified distribution, we use the Anderson–Darling (AD) two-tailed test (Anderson & Darling 1952). It was proven by Engmann & Cousineau (2011) that the AD test is more powerful for comparing distributions than the alternative Kolmogorov-Smirnov (Kolmogorov 1933; Smirnoff 1939) test in detecting any kind of difference between samples from two different distributions. Additionally, the AD test requires less data than the KS test for obtaining sufficient statistical power (Engmann & Cousineau 2011). The null hypothesis that two samples come from the same parent distribution is rejected if AD statistic is larger than the corresponding critical value at a given significance level α (Scholz & Stephens 1987) or, equivalently, if the p-value $< \alpha$. According to standards for statistical evidence, suggested by Johnson (2013), test results are considered to be highly significant for those p-values that are less than $\alpha = 0.001$.

[2] http://www2.lowell.edu/~grundy/tnbs/
[3] http://www.minorplanetcenter.net/iau/lists/MPLists.html

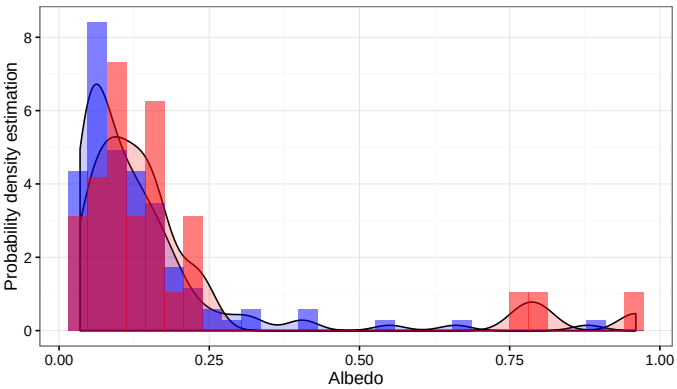

Fig. 1. Empirical albedo distributions of multiple and single TNOs. Red and blue histograms are constructed from the TNBs and TNOs datasets respectively. The solid lines mean the probability density functions estimation (kernel estimation, Parzen 1962), shaded in red and blue for the TNBs and TNOs datasets respectively.

Table 2. Result of the two-tailed AD test applied to diameter dataset using the whole MPC list.

Samples (binaries/non-binaries)	p-value[b]		
	μ	μ+sd	μ−sd
Full dataset (78/2449)	$<10^{-10}$	$<10^{-10}$	$<10^{-5}$
According to dynamical groups[a] :			
(a) only CC (35/546)	0.0004	$<10^{-5}$	0.0028
(b) only HC (19/636)	0.0006	0.0001	0.003
(c) only Det. and SDO (7/325)	0.08	0.03	0.19
(d) only Res. (17/586)	0.0002	$<10^{-5}$	0.0009
Equal size ranges between two samples (61/1235)[c]	0.2	0.09	0.54
Only TNOs with $D < 1142$ km (75/2442)[c]	$<10^{-5}$	$<10^{-5}$	$<10^{-5}$
Only TNOs with $D > 140$ km (63/1215)[c]	0.04	0.01	0.14

Notes. [(a)] Classification of Gladman et al. (2008). CC denotes cold-classicals, HC denotes hot-classicals, Det. and SDO denote detached and scattered disc objects, Res. denotes resonant objects. [(b)] The p-value is computed using the techniques developed by Scholz & Stephens (1987). μ and $\mu\pm$ sd denote p-values, calculated for the mean and mean ± standard deviation of the AD statistic, respectively. [(c)] The average number of objects. The number of objects with $D > 140$ and/or $D < 1142$ varies, depending on Monte Carlo samples.

It was mentioned above, that we assume the albedo distribution is not different for binaries and non-binaries. This assumption can be justified by the AD test result p-value = 0.13, applied to samples from "TNOs are cool" program, which contains albedos for 108 single and 30 multiple objects. This fact indicates, that there is no occurred statistically significant difference between TNOs and TNBs albedo samples. The empirical albedo distributions are shown in Fig. 1.

The resulting p-value for the average AD test statistic for diameter samples is summarised in Table 2. The obtained result (p-value $< 10^{-10}$, i.e. statistical significance $>6.4\sigma$) indicates that the null hypothesis about identical diameter distributions is rejected. However, this result may be biased. To check for biases in statistical conclusions, we have repeated the AD test for different sub-samples. In a first step, the comparison is made for

dynamically equivalent samples, namely using the classification of Gladman et al. (2008; see Table 2). The test statistic shows no significant evidence of the difference between TNBs and TNOs among detached objects and SDO (p-value = 0.08). Thus, it appears that the occurred difference in diameter distributions can be caused by cold classicals, resonant objects, and possibly by cenataurs among which no binaries were observed. On the other hand, this conclusion can be not very robust from statistical point of view, since the small sizes of certain sub-samples for binary objects (e.g. less than 30 binary objects for HC, resonants, detached and SDOs) .

It should be noticed, however, that the compared samples have significantly different size ranges. On the one side, the sample includes a very low binary fraction of small objects among plutinos, SDOs and centaurs. On the other side, the largest objects in the sample – dwarf planets – almost all have satellites. Consequently, the size distribution of TNBs may be biased towards the largest objects, whereas the sample of single TNOs may be biased by small objects. Thus, in a second step, we compare the size distribution over a restricted size range, namely, over the range from 140 km (the diameter of the smallest TNB 2001 RZ143 with known D observed by *Herschel*) to 1142 km (the largest TNO 2007 OR10 without satellites in the *Herschel* sample). In this case, the test indeed shows no significance about difference between two samples. This result indicates that the size difference between the binaries and single samples is biased by small and/or very large TNOs. In order to clarify which objects influence more the statistics, the AD test is repeated for sub-samples without the largest objects, and without the smallest ones. For this purpose we consider, firstly, only objects smaller than 1142 km in diameter, and, secondly, only objects greater than 140 km. The largest known TNOs are the dwarf planets – Haumea, Makemake and Eris. Excluding those objects, the test statistic still shows strong difference in size distributions (p-value $< 10^{-5}$, i.e. statistical significance $>4.3\sigma$). On the other hand, excluding TNOs smaller than 140 km in diameter, the difference between samples is not significant any more (p-value = 0.04). Therefore, the small objects are the ones that bias the test when all size ranges are considered simultaneously.

Using the entire MPC list, however, may not be completely representative of the "TNOs are cool" sample from which the albedo distribution was derived. Indeed the "TNOs are cool" sample was selected back in 2007–2008 (with a few replacement targets introduced at a later stage). It is known that the quality of the MPC information (H_V magnitudes in particular) has been constantly improving over the years. A second aspect is that the MPC database includes objects for which we do not know if they are binaries or not. The fraction of known binaries decreases as the objects get fainter. The faintest MPC binary 2003 TJ58 has magnitude $H_V = 8$. Hence, to adopt a MPC list more representative of the "TNOs are Cool" sample and to avoid objects of uncertain single vs. binary nature, we repeat the same statistical testing, but now we only select 1089 objects from MPC, discovered before 2008 and brighter than $H_V = 8$. This approach allows us to reduce possible discovery biases inherent to the MPC database list.

The obtained results with the reduced MPC list, which consists of 78 binaries and 1011 single objects, are summarised in Table 3. The test statistic (p-value $< 10^{-7}$, i.e. statistical significance $>5.2\sigma$) still indicates that the binaries vs. non-binaries populations have different size distributions. The same tendency, as for the whole MPC list, is seen for all sub-samples, except the population of cold classicals where the statistical significance slightly decreases (p-value = 0.005, i.e. statistical significance $>2.6\sigma$). Still, the results indicate that small objects are the ones that bias the test when all size ranges are considered simultaneously.

Table 3. Result of the two-tailed AD test applied to diameter dataset using the reduced MPC list.

Samples[a] (binaries/non-binaries)	p-value[b]		
	μ	μ+sd	μ−sd
Full dataset (78/1011)	$<10^{-7}$	$<10^{-8}$	$<10^{-6}$
According to dynamical groups[a] :			
(a) only CC (35/369)	0.005	0.0006	0.02
(b) only HC (19/274)	0.0008	0.0002	0.004
(c) only Det. and SDO (7/90)	0.06	0.02	0.18
(d) only Res. (17/251)	0.001	0.0002	0.006
Equal size ranges between two samples (61/617)[c]	0.01	0.002	0.07
Only TNOs with $D < 1142$ km (75/1009)[c]	$<10^{-5}$	$<10^{-6}$	0.0002
Only TNOs with $D > 140$ km (64/615)[c]	0.002	0.0002	0.014

Notes. [(a)] Classification of Gladman et al. (2008). CC denotes cold-classicals, HC denotes hot-classicals, Det. and SDO denote detached and scattered disc objects, Res. denotes resonant objects. [(b)] The p-value is computed using the techniques developed by Scholz & Stephens (1987). μ and $\mu\pm$ sd denote p-values, calculated for the mean and mean ± standard deviation of the AD statistic, respectively. [(c)] The average number of objects. The number of objects with $D > 140$ and/or $D < 1142$ varies, depending on Monte Carlo samples.

To sum up, the difference in size distribution is biased by small TNOs, among which no binaries are observed. Thus, it is likely, that if the small TNBs could be observed, the size distribution between TNBs and single TNOs would not be different.

4. Effective diameters and densities

The analysis of size and density is of particular interest. It may lead to a better understanding of which one of two scenarios is more likely: (a) that small TNOs have been building blocks for bigger ones, in which case there would be a correlation between diameter and density and the increase in density would be caused by less porosity and gravitational compaction while maintaining ice/rock ratio; or (b) there is a clear difference in the densities of large TNOs compared to moderate-sized ones, which implies different formation locations or epochs (Brown 2013). The limit in diameter between the two regimes is somewhere between 500−800 km diameter but there is only one object with a known density (2002 UX25; Brown 2013).

The radiometric diameter for multiple systems is an effective diameter that means $D = \sqrt{D_1^2 + D_2^2}$ for binary system and $D = \sqrt{D_1^2 + D_2^2 + D_3^2}$ for triple system, with D_i the diameter of the ith component.

We have estimated the bulk density for those objects whose mass is available. Thus, assuming identical albedo and identical density for all components of multiple system, and supposing all components are spherical, the bulk density is calculated from the given effective diameter D, the mass of multiple system m and the magnitude difference ΔH_V, by the formula $\rho_b = \frac{6m}{\pi D'^3}$, where

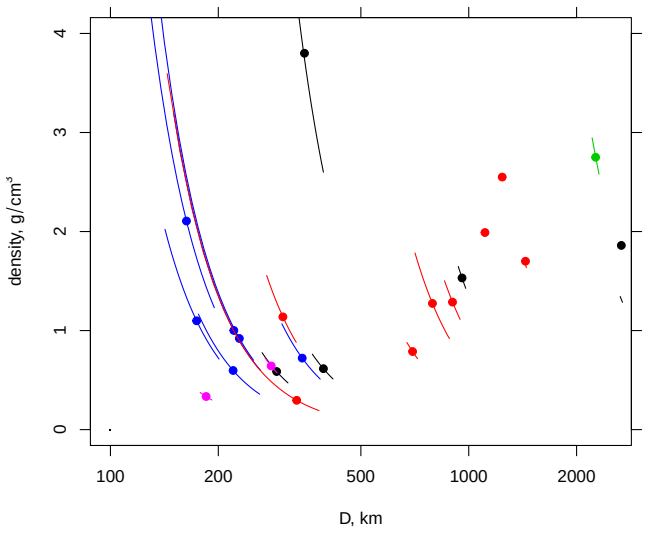

Fig. 2. Effective diameter, D, vs. bulk density for observed TNBs. Blue symbols – cold classicals, red symbols – hot classicals, black symbols – resonants (including plutinos), magenta symbols – scattered disc objects, green symbols – detached objects.

$D' = \frac{(1+k^3)^{1/3}}{\sqrt{1+k^2}} D$ and $D' = \frac{(1+k_1^3+k_2^3)^{1/3}}{\sqrt{1+k_1^2+k_2^2}} D$ for binary and triple system, respectively. The diameters ratio is $k = D_2/D_1 = 10^{-0.2\Delta H_V}$ (assuming equal albedos), and consequently, for triple system $k_1 = D_2/D_1$ and $k_2 = D_3/D_1$.

To the best of our knowledge the calculated ρ_b densities of 2005 EF298 and 2002 WC19 are presented here for the first time. The densities for other objects coincide with previously published papers (Vilenius et al. 2014; Ortiz et al. 2012; Fornasier et al. 2013; Mommert et al. 2012; Santos-Sanz et al. 2012; Lellouch et al. 2013; Sicardy et al. 2011; Braga-Ribas et al. 2013). It should be noted that among all objects in our dataset 2002 WC19 has an exclusively high density. While, with a nominal diameter of 348 km and density of 3.74 g/cm^3, it appears to be an outlier in the density-diameter plot (Fig. 2), we note that error bars on the density are very large and dominated by the +/−13% error on the diameter. Improved diameter and mass determinations are needed for this object.

We have adopted published ρ_b of Haumea and Quaoar, which were derived without assumption about sphericity of the object. The shape of Haumea was constrained from rotational light curves (Lacerda & Jewitt 2007). The Quaoar's density was derived by Braga-Ribas et al. (2013), assuming a Maclaurin spheroid form with an indeterminate polar aspect angle.

We explored the sensitivity to our assumption of identical albedos by postulating that one of the two objects has an albedo 50% greater than that of the other (a similar approach was used by Grundy et al. 2015). Thus, firstly, we assumed that secondaries have higher albedos. This assumption gives smaller bulk densities (see Table 4). Secondly, we assumed that primaries have higher albedos and obtained the opposite effect (greater densities) for all objects except 2001 QY297, Sila and Quaoar. In any case, the bulk densities do not change dramatically. Thus, uncertainties in density related to possible albedo differences between the primary and secondary are dwarfed by uncertainties due to system equivalent diameter and mass.

Table 4. Influence of different albedos of binary components on bulk density.

Object	ρ_b, g/cm^3	$\rho_{b,1}$, g/cm^3	$\rho_{b,2}$, g/cm^3
2001 QY297	$0.920^{+1.31}_{-0.27}$	$0.896^{+1.28}_{-0.27}$	$0.919^{+1.31}_{-0.27}$
2001 XR254	$1.0^{+0.98}_{-0.57}$	$0.96^{+0.94}_{-0.55}$	$1.02^{+0.99}_{-0.58}$
Borasisi	$2.11^{+2.58}_{-1.26}$	$2.03^{+2.48}_{-1.21}$	$2.14^{+2.62}_{-1.28}$
Teharonhiawako	$0.60^{+0.37}_{-0.34}$	$0.57^{+0.35}_{-0.33}$	$0.62^{+0.38}_{-0.35}$
2005 EF298	$1.10^{+0.66}_{-0.56}$	$1.05^{+0.68}_{-0.54}$	$1.13^{+0.67}_{-0.58}$
Sila-Nunam	0.73 ± 0.28	0.71 ± 0.27	0.72 ± 0.28
Eris	2.75 ± 0.22	2.75 ± 0.22	2.76 ± 0.22
Salacia	1.29 ± 0.23	1.24 ± 0.22	1.35 ± 0.24
Altjira	$0.30^{+0.51}_{-0.14}$	$0.29^{+0.49}_{-0.14}$	$0.30^{+0.51}_{-0.14}$
Varda	$1.28^{+0.42}_{-0.46}$	$1.21^{+0.4}_{-0.44}$	$1.35^{+0.45}_{-0.48}$
Quaoar	1.99 ± 0.46	1.96 ± 0.32	1.97 ± 0.32
2002 UX25	$0.78^{+0.10}_{-0.1}$	$0.76^{+0.1}_{-0.09}$	$0.81^{+0.11}_{-0.1}$
2001 QC298	$1.14^{+0.35}_{-0.32}$	$1.09^{+0.34}_{-0.31}$	$1.15^{+0.36}_{-0.32}$
Makemake	1.67 ± 0.35	1.66 ± 0.35	1.67 ± 0.35
2002 WC19	3.74 ± 1.7	3.66 ± 1.66	3.85 ± 1.75
1998 SM165	$0.59^{+0.16}_{-0.14}$	$0.57^{+0.15}_{-0.13}$	$0.61^{+0.17}_{-0.14}$
Orcus	1.53 ± 0.12	$1.49^{+0.12}_{-0.12}$	1.59 ± 0.12
1999 TC36	$0.47^{+0.1}_{-0.09}$	$0.45^{+0.1}_{-0.09}$	$0.49^{+0.1}_{-0.1}$
Typhon	0.34 ± 0.05	0.32 ± 0.05	0.35 ± 0.05
Ceto	0.64 ± 0.13	0.61 ± 0.12	0.66 ± 0.13

Notes. $\rho_{b,1}$ means the bulk density calculated with assumption that the secondary has an albedo 50% greater than that of the primary. $\rho_{b,2}$ means the bulk density calculated with assumption that the primary has an albedo 50% greater than that of the secondary.

5. Search for correlations

We examine whether albedo (p_V) and diameter (D) are correlated with the following parameters: total mass of multiple system (m), bulk density (ρ_b), magnitude difference between components (ΔH_V), $V - R$ colour; orbital parameters of heliocentric orbit: semi-major axis (a), eccentricity (e), inclination (i), perihelion distance (q), mean heliocentric distance of observations (r_H); and mutual orbit parameters: semi-major axis (a_r), orbital period (P). For this purpose, the Spearman's rank correlation coefficient (Spearman 1904) is applied.

The Spearman's rank coefficient uncertainty is estimated using the Monte Carlo approach proposed by Curran (2015). This method combines bootstrap/resampling techniques and the perturbation method. For each pair of parameters, 10 000 random datasets were created. Each new data set consists of randomly chosen pairs from the original data, such that some of the original pairs may appear more than once or not at all. Additionally, each pair in a new dataset is perturbed following a normal asymmetric distribution with mean and standard deviation according to the original pair and given uncertainty respectively. In this way, the bootstrap method estimates the error of the correlation coefficient associated with lack of data, whereas perturbation estimates the error of the given data points.

The resulting Spearman's ρ coefficients are listed in Table 5. Considering correlations with p-value less 0.001 as being highly significant (according to Johnson 2013), and classifying correlations by ρ-coefficient $0.6 \leq |\rho| \leq 1$ as a strong correlation, the test gives (see Table 5, bold text) the highly significant evidence

Table 5. Summary of correlations with diameter and geometric albedo for the multiple TNOs sample.

Parameters	N	Spearman's-ρ	$\pm\varepsilon$	p-value
$\boldsymbol{D}$ vs. $\boldsymbol{m}$	21	0.93	0.06	1.32×10^{-9}
$\boldsymbol{D}$ vs. $\boldsymbol{i}$	30	0.72	0.11	7.73×10^{-6}
$\boldsymbol{D}$ vs. $\boldsymbol{\Delta H_V}$	30	0.66	0.12	7.19×10^{-5}
D vs. ρ_b	21	0.45	0.25	0.04
D vs. ρ_b^*	20	0.49	0.26	0.029
D vs. a_r	21	0.06	0.29	0.79
D vs. e	30	0.25	0.18	0.18
D vs. P	21	−0.34	0.22	0.13
D vs. a	30	−0.06	0.2	0.76
D vs. q	30	−0.29	0.17	0.12
D vs. r_h	29	0.52	0.16	0.13
D vs. $V-R$	24	−0.28	0.23	0.18
p_V vs. m	21	0.43	0.24	0.05
p_V vs. i	30	0.06	0.23	0.76
p_V vs. ΔH_V	30	0.37	0.19	0.07
p_V vs. ρ_b	21	0.58	0.2	0.006
p_V vs. ρ_b^*	20	0.56	0.22	0.009
p_V vs. a_r	21	−0.01	0.29	0.97
p_V vs. e	30	0.01	0.21	0.98
p_V vs. P	21	−0.02	0.25	0.94
p_V vs. a	30	0.13	0.21	0.49
p_V vs. q	30	0.12	0.2	0.52
p_V vs. r_h	29	0.48	0.19	0.26
p_V vs. $V-R$	24	−0.21	0.25	0.31
m vs. ρ_b	21	0.58	0.23	0.01
m vs. ρ_b^*	20	0.56	0.21	0.01
D vs. p_V	30	0.18	0.23	0.33

Notes. Significant correlation are marked as bold in the text. ρ_b^* denotes the bulk densities dataset excluding 2002 WC19. D_1 denotes the primary's diameter. N is the size of the dataset, Spearman's-$\rho \pm \varepsilon$ is the Spearman's rank coefficient with the error estimate by Curran (2015) method, the p-value is calculated for null hypotheses: Spearman's-$\rho = 0$.

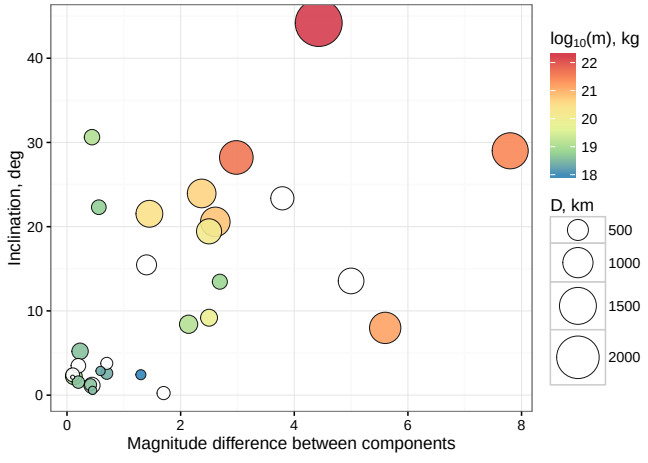

Fig. 3. Strong correlations for binary TNOs: diameter vs. inclination, diameter vs. magnitude difference ΔH_V and diameter vs. total mass of multiple system, m. White circles represent objects with unknown mass.

of the following strong correlations of: D vs. m, D vs. i, and D vs. ΔH_V.

Figure 3 shows the three strongest correlations with diameter. On the figure it can be noticed a trend to have small objects concentrated in the part of low inclination with small magnitude differences (left-bottom part of the plot) whereas large massive objects are dispersed with higher inclinations and greater magnitude differences.

5.1. Diameter, mass and bulk density

The strong correlation between diameter and the total mass of multiple system is a trivial consequence of the fact that the mass is proportional to the total volume (i.e. D^3). Mass also depends on the density, but the Spearman's-ρ test shows the correlation between mass and diameter to be much stronger than the one between mass and bulk density (see Table 5). Therefore, the density influences to the total mass less than the diameter.

Previous papers (Brown 2012; Vilenius et al. 2014; Fornasier et al. 2013; Stansberry et al. 2012) noted the trend that small TNBs have low densities, while larger ones have increasingly higher densities. In this work, the statistical test shows only moderate significance of correlation between the diameter and bulk density (Spearman's-$\rho = 0.45$, p-value $= 0.04$, i.e. statistical significance 1.8σ). The following scenarios may explain this correlation.

A possible explanation suggests that the low density of small objects is due to high porosity and/or a significant fraction of water ice (Vilenius et al. 2012), whereas the large objects have a rock-rich structure and less porosity. In addition, a self compaction under gravitational stress will also produce higher ρ_b for larger objects. According to this scenario, the large objects have been formed by a coagulation and compression of small objects, followed by significant loss of water ice during accretion (Lupo & Lewis 1979; Brown 2012). Binaries in this scenario may form in collision at low velocity, close to the mutual escape velocities, in which both bodies retain their composition (Brown 2012; Barr & Schwamb 2016). Nonetheless, the process of coagulation seems to be unlikely for explaining the very high density of some objects. For example, Brown (2013) shows that this scenario is not compatible with the TNB 2002 UX25. Thus, another scenario is required to explain the very high densities of certain objects.

The large TNBs, such as Eris, Haumea and Quaoar, which exclusively have high densities, may be formed by giant impacts (Brown & Schaller 2007; Brown et al. 2007; Fraser et al. 2013; Barr & Schwamb 2016). These collisions would have removed a large amount of water ice from a differentiated mantle and produced a dense primary with small icy satellites. However, physical conditions (temperature, velocity) required in this type of collision, resulting such a high density of small satellites, seem to be not realistic in the solar system (Brown 2012; Stewart & Leinhardt 2009).

A moderate correlation occurs between albedo and bulk density ($\rho = 0.58$, p-value $= 0.006$, that is, statistical significance 2.5σ), it is most easily understood as a reflection of, on the one hand, the correlation between density and D, and, on the other hand, the tendency of a volatile ice retention on the more massive objects (Schaller & Brown 2007). No similar direct causal link is expected between albedo and bulk density, so we consider their weak correlation to be incidental.

5.2. Diameter and inclination

The positive correlation between effective diameter, D, and inclination, i, is consistent with general findings on Kuiper belt objects, without regard to whether they are singles or binaries. The first discovery of correlation between size and inclination

was done by Levison & Stern (2001). They inferred it from the correlation between absolute magnitude and i, under assumption that the differences in magnitude are primarily due to size, not albedo. According to Levison & Stern (2001), the interpretation of this correlation is related to the presence of two distinct populations: dynamically excited, or hot, objects with higher inclination and dynamically cold objects with inclination less than 5°. Bernstein et al. (2004), making the inference from the luminosity functions of TNO populations, suggested that the population of hot objects exhibits a different size distribution than the cold population. This finding was supported by Fuentes & Holman (2008), Petit et al. (2011) and Fraser et al. (2014). Furthermore, the total mass of TNOs in populations, estimated with the obtained size distributions in the aforementioned works, also indicates the difference between hot and cold groups. For instance, according to Fraser et al. (2014), the estimated masses of the cold and hot populations are ~3×10^{-4} and ~0.01 Earth masses, respectively. Bernstein et al. (2004) pointed that the hot TNOs population has most of its mass in large objects, so that the brightest TNOs are almost entirely in the hot population. The accretion history of the dynamically excited objects placed a larger fraction of the mass into the largest bodies. This is in agreement with the Nice model (Gomes et al. 2005), where the hot population objects were scattered to their current locations from a region between ~15 and 35 AU. Concerning the dynamically cold population, Levison & Stern (2001) suggested it being a dynamically primordial one. Namely, these objects most likely formed close to where they are observed now and have not been significantly perturbed over the solar system's formation.

Our results are also in agreement with whose obtained in the work of Vilenius et al. (2014), where size distributions were considered for classicals from the "TNOs are cool" dataset (not only binaries). They found correlation D vs. i significant at 4.4σ and showed that it is not a selection bias. In order to explore whether the effective diameter vs. inclination correlation for our binary TNOs sample may be due to a selection bias, we examine the correlation between D and heliocentric distance $r_{\rm H}$ (a selection bias would result in smaller objects being preferentially observed at smaller $r_{\rm H}$), and between $r_{\rm H}$ and i (such a bias, if it existed for some reason, could influence the D vs. i correlation). In neither case do we find evidence of such a bias for the TNBs in our sample. For i vs. $r_{\rm H}$ the Spearman's correlation coefficient is ρ = 0.52, but the significance of it is extremely low (p-value = 0.99). For D vs. $r_{\rm H}$ (see Table 4), ρ = 0.16 and the significance is low (p-value = 0.13). This contrasts, for example, with the strong (ρ = 0.78, p-value < 10^{-7}, i.e. >8σ) correlation between D and $r_{\rm H}$ in the larger sample of 85 binary and single TNOs observed by *Herschel* (Lellouch et al. 2013). These considerations suggest that the positive correlation of D vs. i for our TNBs sample is not a result of selection biases.

5.3. Diameter and magnitude difference

The next strong correlation we found is between D and magnitude difference between binary components, ΔH_V. Usually the albedos cannot be measured individually, so it is assumed that the primary and secondary components have equal albedos (e.g. Noll et al. (2008)). Then the magnitude difference can be related to the primary-to-secondary diameter ratio by $D_1/D_2 = 10^{0.2\Delta H_V}$. The assumption of equal albedos for the binary components seems to be supported by the observation that objects in such systems usually have very similar visible colours (Benecchi et al. 2010). Under this "equal albedos" assumption, the interpretation of the D vs. ΔH_V correlation is that the larger objects have relatively small satellites, while smaller objects are preferentially in systems where the components are more equal in size.

The fact that, generally, the small TNBs have similar in size components and the dwarf planets posses satellites, which are much smaller than the primaries, explains the aforementioned correlation. This trend has been already noted, for example, by Brown et al. (2006), Noll et al. (2008), Nesvorný et al. (2010). This correlation D vs. D_1/D_2 points to a differences between the origins of small and large TNBs.

For binaries with a large primary and relatively small satellite, collisional scenario of formation is more likely. The satellites of the larger objects are assumed to be collisional fragments from the mantle which were ejected from giant impacts. Under this hypothesis, the velocity at the ejection was low enough to stay into an orbit around the primary and to not escape. This scenario explains Eris', Haumea's and Quaoar's satellites formation (Brown & Schaller 2007; Brown et al. 2007; Fraser et al. 2013).

The mid-sized TNBs Varda, Orcus and Salacia have similar orbital characteristics of their satellites (Grundy et al. 2015, 2011; Stansberry et al. 2012), suggesting a common formation history for these systems. These objects are also consistent with formation from a giant impact. However, the colour difference between Orcus and his satellite could indicate a different type of collision (Brown et al. 2010), than those in case of Eris, Haumea and Quaoar. The Orcus formation is more consistent with a relatively slow collision of partly differentiated precursor bodies, similar in character to the Pluto/Charon collision (Canup 2010; Barr & Schwamb 2016).

It is more likely that the small binaries with equal-sized components are outcome of dynamical capture (Astakhov et al. 2005). These mutual capture seems to be the most convenient scenario for many TNBs with high angular momentum. Being very distant from the Sun, these small binaries have a low velocity, and, consequently, a small kinetic energy, that makes such capture possible (Noll et al. 2008). Another possible mechanism of binaries with equal-sized components formation is a gravitational collapse (Nesvorný et al. 2010). According to this scenario, binary systems form in the protoplanetary disks during gravitational collapse when the excess of angular momentum prevented the agglomeration of available mass into a solitary TNO.

Figure 4 shows the ΔH_V vs. D distribution. It can be noticed that there are 2 empty areas in Fig. 4. One of them (top left) may result from discovery bias. Clearly, it is difficult to discover binarity with large ΔH_V when the overall system is faint and small. We note that Fraser et al. (2017) recently discovered 2002 VD131 (H = 6.5) to be a binary system with flux ratio 0.061, that is ΔH_V = 3.03. Although the system albedo is unknown, assuming a 10% value, typical of TNOs, would lead to an equivalent diameter D = 210 km. This would place this object within and near the edge of this area, illustrating that its apparent emptiness in our sample is an observational bias. In contrast, the bottom right empty area is not a bias. In fact, it indicates that large, similar-sized binaries do not exist, i.e. that the Astakhov et al. (2005) model of capture does not work at large sizes.

6. Summary and conclusions

We have analysed albedo/size characteristics of 30 trans-Neptunian multiple objects (28 binary and 2 triple systems),

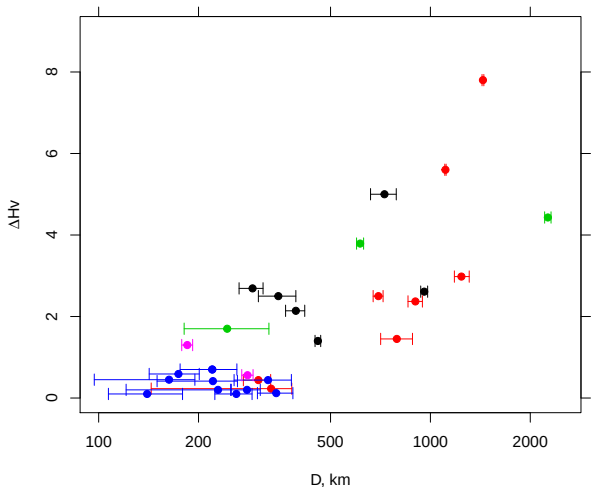

Fig. 4. Correlation of effective diameter D with magnitude difference ΔH_V for observed multiple TNOs. Blue symbols – cold classical TNOs, red symbols – hot classical TNOs, black symbols – resonant TNOs (including plutinos), magenta symbols – scattered disc objects, green symbols – detached TNOs.

observed during the "TNOs are cool" programme. The main results are summarised hereafter:

1. The size distributions of the binary object population and the population of single TNOs have been compared. We have used the MPC database to expand data samples and estimate real size distributions. The test statistic showed that the single vs. multiple populations have different size distributions, but this result is biased due to a lack of discovered binaries among small TNOs.
2. We determined new bulk densities of two binary systems, based on our estimated sizes and published masses: 2005 EF298 ($1.10^{+0.66}_{-0.56}$ g/cm^3) and 2002 WC19 (3.47 ± 1.7 g/cm^3). We note that estimated uncertainties on the density of 2002 WC19 are very large, and require improved diameter and mass determination.
3. We have found three strong correlations of effective diameter with (1) the total mass of binary system; (2) the heliocentric inclination and (3) the magnitude difference between components. The diameter vs. mass correlation is an obvious one, since the effective diameter influences total mass more than the density. The correlation between diameter and inclination is consistent with a previously known trend applying to the trans-Neptunian population as a whole. The correlation between diameter and magnitude difference implies that the small systems have similar in size components, whereas the large ones, as dwarf planets, posses satellites, which are much smaller than the primaries. This correlation is partly the result of an observational bias – the difficulty to detect binaries with large ΔH_V at faint overall magnitude. However the lack of large, similar-sized binaries is not an observational bias. It indicates that large objects possess satellites much smaller than the primaries. This fact may indicate that small and large binaries form through different mechanisms.
4. We have found two possible correlations between diameter and bulk density and between albedo and bulk density. However, the small sample size of accurate densities explains the lower statistical significance of these correlations. These results require a larger dataset in order to be verified.

Acknowledgements. This work is supported by Labex ESEP (ANR N 2011-LABX-030) and German DLR project No. 50 OR 1108. T. Müller acknowledges funding from the European Union's Horizon 2020 Research and Innovation Programme, under Grant Agreement no 687378. I. Kovalenko acknowledges V. V. Emel'yanenko for his helpful discussions.

References

Anderson, T. W., & Darling, D. A. 1952, The annals of mathematical statistics, 193
Astakhov, S. A., Lee, E. A., & Farrelly, D. 2005, MNRAS, 360, 401
Barr, A. C., & Schwamb, M. E. 2016, MNRAS, 460, 1542
Benecchi, S. D., Noll, K., Grundy, W., & Levison, H. 2010, Icarus, 207, 978
Bernstein, G. M., Trilling, D., Allen, R., et al. 2004, AJ, 128, 1364
Braga-Ribas, F., Sicardy, B., Ortiz, J., et al. 2013, ApJ, 773, 26
Brown, M. E. 2012, Ann. Rev. Earth Planet. Sci., 40, 467
Brown, M. E. 2013, ApJ, 778, L34
Brown, M. E., & Schaller, E. L. 2007, Science, 316, 1585
Brown, M., Van Dam, M., Bouchez, A., et al. 2006, ApJ, 639, L43
Brown, M. E., Barkume, K. M., Ragozzine, D., & Schaller, E. L. 2007, Nature, 446, 294
Brown, M., Ragozzine, D., Stansberry, J., & Fraser, W. 2010, AJ, 139, 2700
Canup, R. M. 2010, AJ, 141, 35
Curran, P. A. 2015, Astrophysics Source Code Library, 1, 04008
Engmann, S., & Cousineau, D. 2011, Journal of Applied Quantitative Methods, 6, 1
Fornasier, S., Lellouch, E., Müller, T., et al. 2013, A&A, 555, A15
Fraser, W. C., Bannister, M. T., Pike, R. E., et al. 2017, Nat. Astron., 1, 0088
Fraser, W. C., Batygin, K., Brown, M. E., & Bouchez, A. 2013, Icarus, 222, 357
Fraser, W. C., Brown, M. E., Morbidelli, A., Parker, A., & Batygin, K. 2014, ApJ, 782, 100
Fuentes, C. I., & Holman, M. J. 2008, AJ, 136, 83
Gladman, B., Marsden, B. G., & VanLaerhoven, C. 2008, The Solar System Beyond Neptune, 43
Gomes, R., Levison, H. F., Tsiganis, K., & Morbidelli, A. 2005, Nature, 435, 466
Grundy, W., Stansberry, J., Noll, K., et al. 2007, Icarus, 191, 286
Grundy, W., Noll, K., Nimmo, F., et al. 2011, Icarus, 213, 678
Grundy, W., Benecchi, S., Rabinowitz, D., et al. 2012, Icarus, 220, 74
Grundy, W., Porter, S., Benecchi, S., et al. 2015, Icarus, 257, 130
Grundy, W., Binzel, R., Buratti, B., et al. 2016, Science, 351, 9189
Harris, A. W. 1998, Icarus, 131, 291
Johnson, V. E. 2013, Proc. National Academy of Sciences, 110, 19313
Kolmogorov, A. N. 1933, Foundations of probability
Lacerda, P., & Jewitt, D. C. 2007, AJ, 133, 1393
Lebofsky, L. A., Sykes, M. V., Tedesco, E. F., et al. 1986, Icarus, 68, 239
Lellouch, E., Santos-Sanz, P., Lacerda, P., et al. 2013, A&A, 557, A60
Lellouch, E., Santos-Sanz, P., Fornasier, S., et al. 2016, A&A, 588, A2
Levison, H. F., & Stern, S. A. 2001, AJ, 121, 1730
Lupo, M. J., & Lewis, J. S. 1979, Icarus, 40, 157
Mommert, M. 2013, Ph.D. Thesis, Freie Universität Berlin
Mommert, M., Harris, A., Kiss, C., et al. 2012, A&A, 541, A6
Müller, T. G., Lellouch, E., Böhnhardt, H., et al. 2009, Earth Moon and Planets, 105, 209
Nesvornỳ, D., Youdin, A. N., & Richardson, D. C. 2010, AJ, 140, 785
Noll, K. S., Grundy, W. M., Chiang, E. I., Margot, J.-L., & Kern, S. D. 2008, Binaries in the Kuiper Belt, eds. M. A. Barucci, H. Boehnhardt, D. P. Cruikshank, A. Morbidelli, & R. Dotson, 345
Ortiz, J., Sicardy, B., Braga-Ribas, F., et al. 2012, Nature, 491, 566
Parker, A. H., Buie, M. W., Grundy, W. M., & Noll, K. S. 2016, ApJ, 825, L9
Parzen, E. 1962, Ann. Math. Stat., 33, 1065
Petit, J.-M., Kavelaars, J. J., Gladman, B. J., et al. 2011, AJ, 142, 131
Pilbratt, G. 2008, in COSPAR Meeting, Vol. 37, 37th COSPAR Scientific Assembly, 2437
Ragozzine, D., & Brown, M. E. 2009, AJ, 137, 4766
Santos-Sanz, P., Lellouch, E., Fornasier, S., et al. 2012, A&A, 541, A92
Schaller, E. L., & Brown, M. 2007, ApJ, 659, L61
Schindler, K., Wolf, J., Bardecker, J., et al. 2017, A&A, 600, A12
Scholz, F. W., & Stephens, M. A. 1987, J. Am. Statist. Assoc., 82, 918
Sicardy, B., Ortiz, J., Assafin, M., et al. 2011, Nature, 478, 493
Smirnoff, N. 1939, Matematicheskii Sbornik, 48, 3
Spearman, C. 1904, Amer. J. Psych., 15, 72
Stansberry, J., Grundy, W., Brown, M., et al. 2008, The Solar System Beyond Neptune (Tuscon: University of Arizona Press), 161
Stansberry, J., Grundy, W., Mueller, M., et al. 2012, Icarus, 219, 676
Stern, S., Bagenal, F., Ennico, K., et al. 2015, Science, 350, 1815
Stewart, S. T., & Leinhardt, Z. M. 2009, ApJ, 691, L133
Vilenius, E., Kiss, C., Mommert, M., et al. 2012, A&A, 541, A94
Vilenius, E., Kiss, C., Müller, T., et al. 2014, A&A, 564, A35
Weaver, H., Buie, M., Buratti, B., et al. 2016, Science, 351, 0030